Lasers in Manufacturing Conference 2017

Laser-micro-processing with ultrashort pulses using flexible beam delivery

B. Jaeggi[a,*], B. Neuenschwander[a], S. Remund[a], S. Eilzer[b], M. C. Funck[b], B.Wedel[b]

[a]*Bern University of Applied Sciences, Institute for Applied Laser, Photonics and Surface Technologies, Pestalozzistrasse 20, 3400 Burgdorf, Switzerland*
[b]*PT Photonic Tools GmbH, Johann-Hittorf-Strasse 8, 12489 Berlin, Germany*

Abstract

Hollow core and kagome photonic crystal fibers offer the possibility to guide ultrashort laser pulses of high energy and average power. They could represent a valuable tool for the power transport from the laser source to the processing unit and would therefore facilitate the integration of ultrashort pulsed laser systems. Many works dealt with the characterization of such fibers concerning beam quality, transmission, polarization etc. when the fiber is in a static position. We combine such a fiber with a femtosecond laser system and our synchronized galvo scanner setup and investigate the influence of a dynamic movement of the fiber. Beside the characterization of the output beam we also demonstrate its influence onto the machining quality for the applications 3D-surface structuring and multi-pulse drilling on the fly. Especially the latter application should be very sensitive to any variations of the beam pointing and polarization.
The experiments demonstrate the applicability of such fibers for its integration in an industrial environment for laser micro-processing.

Keywords: hollow core fiber; kagome fiber; static and dynamic mode; galvo scanner; laser-micro-machining

1. Introduction

Ultrashort laser pulses have shown their applicability for high quality laser micro-machining of metals, semiconductors and insulators in manifold applications. However, to really enter into the large field of

* Corresponding author. Tel.: +41 34 426 41 93
E-mail address: beat.jaeggi@bfh.ch

industrial applications the demand of high throughput and simple beam guiding systems still represent key factors. In the high power cw market the development and introduction of reliable fiber based beam delivery boosted the utilization of such high power lasers as a tool because it enabled flexible beam routing, energy sharing and higher safety during use. But for a long time fiber delivery was almost unthinkable for ultrashort pulses of relevant pulse energies used for laser micro-processing. Photonic crystal fibers PCF allowed to enlarge the core radius by maintaining the single mode beam guiding and could be used to amplify or transport pulses of several 10ps pulse duration at moderate energies. The step to shorter pulses and high pulse energies was offered by hollow core photonic crystal fibers HC-PCF's. In 2007 Tauer et al. reported coupling efficiencies of more than 80% for 10ns pulses at 1064nm wavelength with energies higher than 1mJ when the air pressure in the fiber was reduced to 450mbar. In the same year Gérôme et al. reported about the compression of unchirped single mode 195fs input pulses @ 800nm wavelength to less than 100fs propagation through 8m of fiber, at pulse energies of around 50nJ. Beam delivery of mJ-level fs pulses was then reported by Debord et al. in 2014 for a hypocycloid core-shaped HC-PCF. For a 19-cell fiber filled with Helium and applying 600fs pulses of 1mJ pulse energy a total transmission of about 65% and 57% was reported for a fiber length of 3m and 10m, respectively. In the same work it was shown, that the bending losses increases from about 2dB/km up to 15.5dB/km when the bending radius is decreased from about 9cm down to 6cm. Finally the delivered output of this fiber was directly used for laser micro-machining and micro-graving on several materials with no focusing lens.

Recently HC-PCF's were tested with modern industrial ultrashort pulsed high power systems. Baumbach et al., 2017 reported a transmission of about 90% even for fs-pulses @ 1030nm wavelength above 100W of average power and 200MW peak power. The polarization extinction ratio amounted 20dB up to an average power of 50W. Eilzer et al., 2016 reported on an industrial beam delivery system and also analyzed the polarization behavior for 400fs pulses at 50µJ in different bending situations which has only a small influence. This fiber system was later tested by the same group (Eilzer et al., 2017) in real micro-machining applications where no significant difference to the machining results with a free space beam path was observed.

However, all these experiments were performed with a static fiber position, i.e. the fiber was statically positioned during the experiments. But many machine concepts and applications demand a dynamically moved fiber. Even this movement may be slow, its influence has to be tested. This work reports now about the influence of the motion of the fiber onto polarization, beam pointing and machining results.

2. Experimental Setup

2.1. Beam delivery system

The beam delivery system consists of three main parts:

- The beam launching system (BLS), to couple the laser beam into the fiber. With the BLS, the beam alignment, the mode-field diameter and the focus position can be controlled precisely to achieve optimal coupling conditions. This is necessary to avoid damage of the fiber at higher pulse energies.
- The laser light cable (LLK), which is responsible for the flexible transport of the light from the BLS to the working station. On both ends of the laser light cable a connector is mounted to easily replace the cables.
- The collimation module, to collimate the output beam of the fiber. This module consists of a f=150mm lens, resulting in a beam diameter of about 6mm.

2.2. Experimental Setup in general

For the experiments a Satsuma HP2 from Amplitude Systèmes was used at 1030nm wavelength. The pulse duration at the output of the laser system was 320fs (fit: $sech^2$). The used repetition frequency was 505kHz. The beam was guided through an external attenuator consisting of a polarizer, a $\lambda/2$-waveplate and two folding mirrors. After passing the two mirrors the beam enters the beam launching system (BLS) which is located about 1.2m away from the output aperture of the laser system. In a real application the beam launching system would be placed direct in front of the laser system, as shown in Figure 6 in Funck et al., 2017. The used laser light cable in the experiments has a mode-field diameter of 40µm and a length of 3.5m. The air pressure in the hollow core fiber was reduced to around 15mbar. For a defined movement of the fiber a linear axis LINAX Lxs200F60 from Jenny-Science was used. The acceleration of the axis was set to $2m/s^2$ and the travel range to 180mm. The velocity of the linear axis was varied between 18mm/s and 200mm/s. The linear axis, on which the fiber was mounted, was placed about 120cm from the end connector of the fiber. As sample material a 2mm thick stainless steel 1.4301 (in US: AISI 304) sheet was used for the 3D-structuring. The surface was polished using a 3µm diamond suspension. In addition a 10µm thick stainless steel 1.4310 (in US: AISI 301) foil was used.

2.3. Setup for Characterization

To characterize the polarization as well as the beam profile and the pointing stability two different setups were used. Fig. 1a shows the setup to characterize the beam profile and the beam pointing stability. The beam was attenuated via two wedge-plates and focused with a *f*=750mm lens. The focusing lens was placed 600mm away from the collimation module. Afterwards the beam profile was captured with a Dataray WinCamD-LCM4C, which was placed in the focal plane.

On the other hand to characterize the polarization after the collimation module the beam was guided via a folding mirror to a *f*=-30mm lens which expands the beam. Afterwards the polarization state of the beam was measured using a polarization analyzer SK010PA-NIR from Schäfter+Kirchhoff (see Fig. 1b). The polarization analyzer software shows the polarization state on the Poincaré-sphere.

2.4. Setup for micro-machining

For the micro-machining experiments two different setups were used. To produce reference samples, the beam was guided after passing the external attenuator, via a few folding mirrors to the beam expander located in front of a galvo scanner. To get circular polarization, a $\lambda/4$-waveplate was introduced in the beam

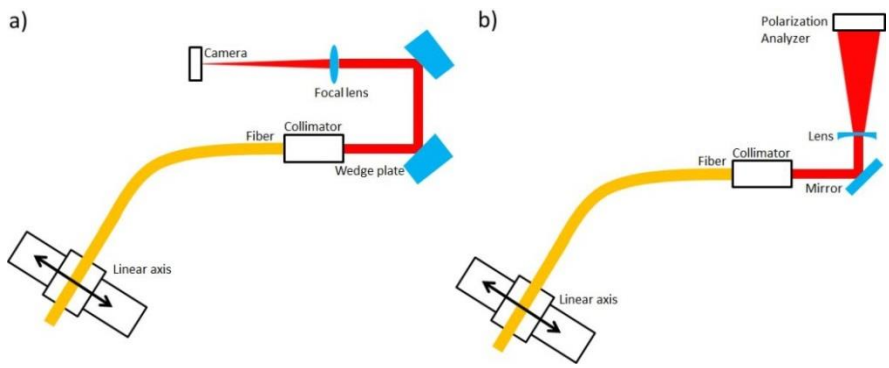

Fig. 1. a) Setup to characterize the beam profile and the beam pointing; b) Setup to characterize the polarization

path as well. The used galvo scanner was an intelli*SCAN*$_{se}$14 from SCANLAB. The beam was focused with a f=160mm objective, resulting in a spot radius w_0 of 17.2µm and a beam quality M^2<1.3.

For the setup using the transportation fiber, the collimation module was directly mounted on the galvo scanner mount, as shown in Fig. 2a,b. In comparison to the setup used for the characterization the fiber was placed in a different way as an additional curve of 90° was introduced. All the bending radii were larger than the allowed minimum amounting 250mm. The influence of the additional bending was not measured. For these experiments a galvo scanner intelli*SCAN*$_{se}$10 from SCANLAB was used. To keep the spot radius in the same range as for the reference tests a telecentric f=100mm objective was used in this case. The polarization after the collimation module was circular as well, adjusted directly in the beam launching system. The galvo scanners were driven in both experimental setups by the own developed synchronization solution shown in Jaeggi et al., 2012 and Zimmermann et al., 2015. The patterns were machined in a raster scanning mode, where the gating information is provided in a b/w-bitmap. Each pixel of the bitmap represents one single laser shot.

3. Characterization of the flexible beam delivery

3.1. Transmission

In a first task the transmission of the beam delivery system was measured. Therefore the average power was measured in front of the beam launching system and after the collimation module. In Fig. 3 the transmission curve over the full power range of the used laser system is shown. The transmission amounts 93%, which is in the specified range of 93%±3% for a 10m long fiber shown in the spec sheet of the fiber on the homepage of Photonic Tools GmbH, and is in good agreement with the results obtained in Eilzer et al., 2016 using similar equipment.

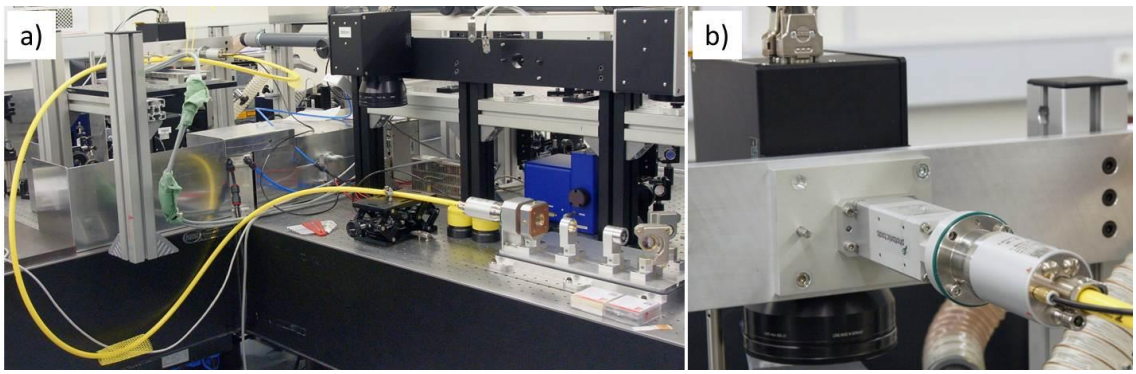

Fig. 2. a) Photograph of the setup for the micro-machining experiments; b) Detail view on the mounting of the collimation module and the galvo scanner

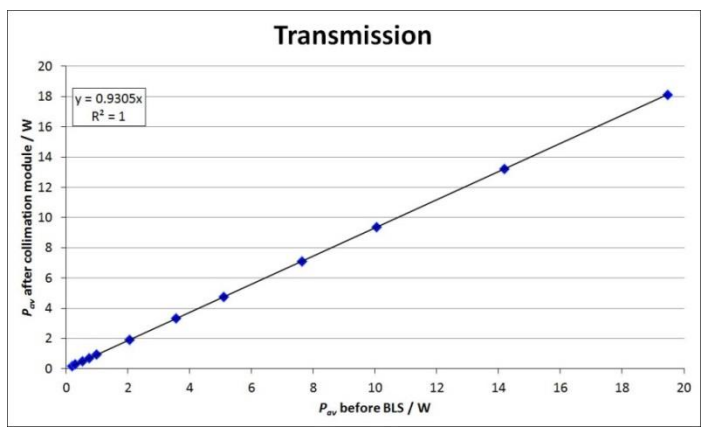

Fig. 3. Transmission of the fiber delivery system, including the beam launching system, the laser light cable and the collimation module

3.2. Polarization

In a next step, the polarization was investigated. First the polarization was measured without a movement of the fiber, see Fig. 4a. In the static mode the polarization is perfectly circular, indicated by the blue points near the R in Fig. 4a, which means circular polarized light in a clockwise direction. Afterwards the fiber was moved with the linear axis. As shown in Fig. 4b, the polarization changes slightly over the traveling distance of the linear axis. The small changes in polarization are in good agreement with the observation in Eilzer et al., 2016.

3.3. Beam profile and beam pointing stability

The beam profile and the beam pointing stability were measured in the focal plane of the *f*=750mm lens. In a first task, the beam pointing was measured without a movement of the fiber, shown as blue diamonds in Fig. 5. The measured beam pointing after the fiber is similar to the beam pointing of today's industrial laser

systems, as shown in Pricking et al., 2016 and Baumbach et al., 2017. Afterwards the fiber was moved using the linear axis at a velocity of 50mm/s. The various beam pointing will lead to a position deviation in the focal plane during micro-machining.

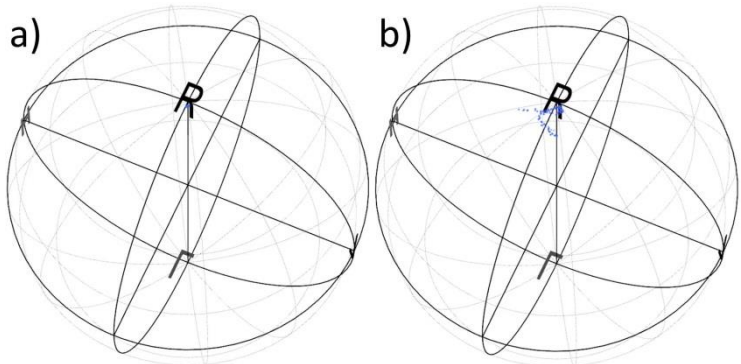

Fig. 4. a) Polarization for the fiber in static mode; b) Polarization for the fiber in dynamic mode with v=100mm/s

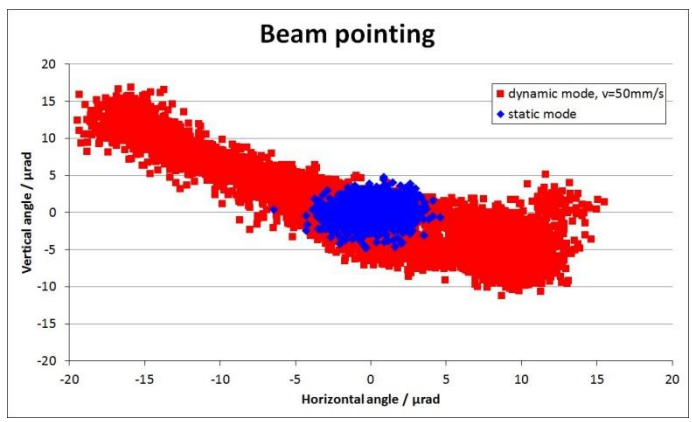

Fig. 5. a) Beam pointing stability measurement for the fiber in static and dynamic mode

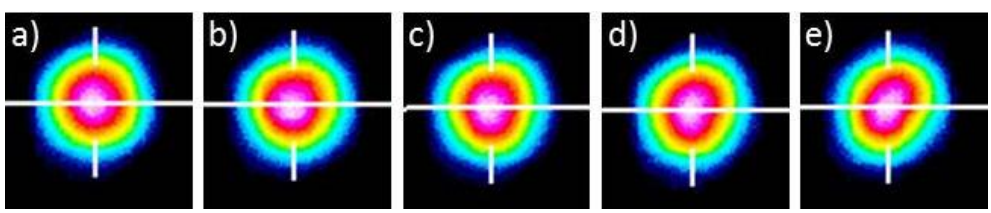

Fig. 6. a) Beam profile for the fiber in static mode, $2 \cdot w_0 \approx 250\mu m$; b) to e) Beam profile for the fiber in motion, captured at different positions of the linear axis, $2 \cdot w_0 \approx 250\mu m$

For the presented micro-machining experiments a *f*=100mm objective was used. For this objective the position deviation can be calculated and amounts ±0.5µm in the static mode and ±1.75µm in the dynamic mode. Not only the beam pointing is of interest, but also the beam profile. As long as the fiber is used in the static mode, the beam profile rest stable. If the fiber is moved, also the beam profile changes slightly. Fig. 6a shows the beam profile for the fiber in static mode and additionally some profiles captured during the motion of the linear axis (Fig. 6b-e). The change of the beam profile seems only to be minimal and its influence during the movement of the fiber has to be investigated for real micro-machining applications.

4. Micro-machining results

4.1. 3D-structuring

In a first step a shark skin like surface structure was produced to see the influence of the fiber onto the surface quality and the surface profile. The peak fluence was chosen to work near the optimum point, where the ablation process is most efficient shown in 2010 by Raciukaitis et al. and Neuenschwander et al. The used peak fluence amounts 0.41J/cm^2. The 3D-structure is divided in 234 different layers. The pitch, meaning the distance between two consecutive pulses in both lateral directions amounts 8.6µm. With the repetition frequency of 505kHz, the corresponding scan speed is 4.343m/s. As already mentioned, in a first step a reference structure was produced without the fiber delivery (Fig. 7a). The same structure was then machined using the fiber delivery in static mode and in dynamic mode with different velocities of the linear axis (Fig. 7b-e). For the velocities of 18mm/s, 50mm/s and 200mm/s no difference to the reference structure or the structure machined with the fiber in static mode can be observed. For 100mm/s speed (Fig. 7e) of the linear axis the situation is different. One cycle of the linear stage takes 3.7s. After this cycle time, the linear axis is at the same position as before. This cycle time is almost equal to the time needed to mark one layer of the 3D-structure, which amounts 3.603s. Therefore the polarization and beam profile at a certain position on the workpiece are slightly shifted from one to the next layer, which lead to the observed structure. The difference between the brighter and the darker parts inside the structure is caused by the existence of well oriented surface ripples. These ripples are known as laser induced periodic surface structures LIPSS (Bonse et al., 2014).

The ripple structure observed on the reference structure (Fig. 8a) and for the fiber in static mode (Fig. 8b) disappears for the dynamic mode where the fiber is moved (Fig. 8c,d,f). The surface morphology is averaged because the polarization slightly changes for a certain position from layer to layer. The only exception is the case when the fiber is moved with 100mm/s as shown in Fig. 8e. On the left hand side of Fig. 8e horizontally oriented ripples exist, where on the right hand side no oriented ripple structure can be observed as for the other velocities of the linear axis. This regular change finally leads to the pattern observed in Fig. 7e. It has to be mentioned here that this is mainly a visual effect, as all topographic measurements using a white light interferometric microscope show similar shapes of the structure and also similar ablation depths.

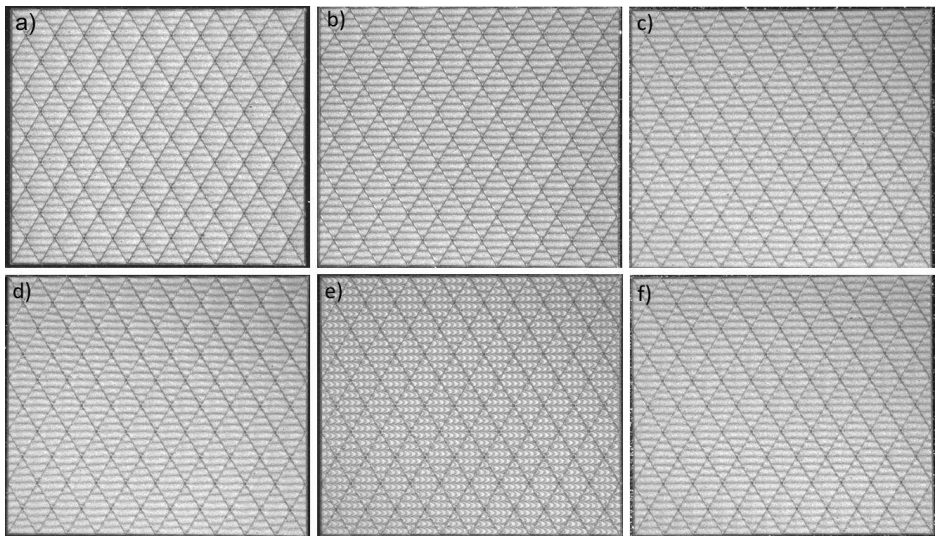

Fig. 7. Shark skin structure for different cases, size of the structure: 5.38x4.36mm; a) reference structure; b) fiber in static mode c) fiber in dynamic mode with 18mm/s; d) 50mm/s; e) 100mm/s; f) 200mm/s

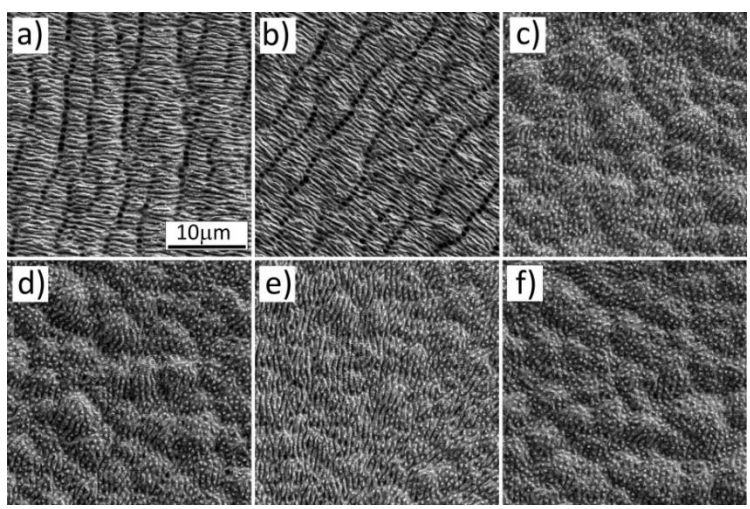

Fig. 8. SEM images of the shark skin surfaces for different cases, SE2-detector; a) reference structure; b) fiber in static mode c) fiber in dynamic mode with 18mm/s; d) 50mm/s; e) 100mm/s; f) 200mm/s

4.2. Multi-pulse on the fly

In the last experiment the influence of the beam pointing variation onto the position accuracy and the shape of drilled holes is investigated. The holes were drilled in a multi-pulse drilling on the fly process. For all layers a single laser shot is applied at each hole position during full motion of the galvo scanner. Each hole position is reached with a accuracy better than 1µm for each layer. If the changes of the beam profile, the

pointing stability or the changes in polarization will have an influence, the shape of the holes should change in the dynamic mode compared to the static mode. The holes were drilled with a pulse energy of 33.4µJ and 300 layers. The hole spacing amounts 50µm. To work with a suitable scan speed of the galvo scanner only every 25th pixel is marked, i.e. between two holes, 24 laser pulses are faded out and sent to the beam dump and not to the sample. Applying this method the scan speed amounts 1.1m/s. Between the holes drilled with the fiber in static mode (Fig. 9b) and the holes machined with the fiber in motion (Fig. 9c-f), no difference in size and shape can be observed on the SEM images. The reference holes drilled with the standard setup without fiber delivery (Fig. 9a) seems to have a slightly larger output diameter. This can be caused by a slightly different beam caustic or a slightly larger beam radius compared to the fiber based machining.

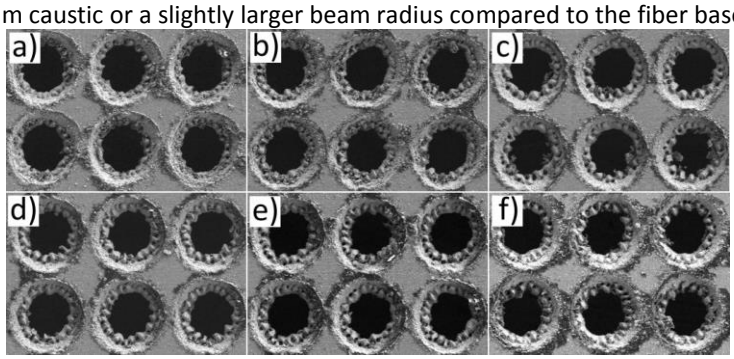

Fig. 9. SEM images of the drilled holes with a hole spacing of 50µm, SE2-detector; a) reference structure; b) fiber in static mode c) fiber in dynamic mode with 18mm/s; d) 50mm/s; e) 100mm/s; f) 200mm/s

5. Conclusions

The measurements and the machining experiments show no difference between the standard setup, where the beam is guided via folding mirrors and the fiber setup used in static mode. If the fiber is used in a dynamic mode, the measurements show an influence on the beam pointing and on the polarization as well. Both parameters slightly changes while the fiber is moved with the linear axis. It has been shown that these small changes do not affect the multi-pulse drilling on the fly process which acts as a benchmark process for this mode. The drilled holes look similar to the holes drilled with the fiber in static mode. Moving the fiber during processing can be used to suppress LIPSS or generate LIPSS with specific orientation direction, which leads to special visual properties of the workpiece. Except for some special processes, for example shown in Bonse et al., 2017, the contour accuracy is even more important for 3D-structuring. With the used measuring equipment no difference in shape and accuracy was observed. The transportation of ultrashort pulses in a fiber can enhance the reliability of machine solutions for micro-machining and opens the door to large scale applications. Further tests are needed to clarify if the stability of the fiber delivery system differs for other more machine-oriented movements. Therefore the fiber end with the end connector and the collimation module has to be moved in a fix-optic setup or together with the galvo scanner.

Acknowledgements

Special thanks to Josef Zuercher for the help with the SEM images and Urs Hunziker for his work in the mechanical workshop.

References

Baumbach, S., Pricking, S., Overbuschmann, J., Nutsch, S., Kleinbauer, J., Gebs, R. Tan C., Scelle, R., Kahmann, M., Budnicki, A., Sutter, D. H., Killi, A., 2017, Ultra-short pulse delivery at high average power with low-loss hollow core fibers coupled to TRUMPF's TruMicro laser platforms for industrial applications, Proc. of SPIE, Vol. 10094

Bonse, J., Kirner, S. V., Höhm, S., Epperlein, N., Spaltmann, D., Rosenfeld, A., Krüger, J., 2017, Applications of laser-induced periodic surface structures (LIPSS), Proc. of SPIE, Vol.10092

Bonse, J., Koter, R., Hartelt, M., Spaltmann, D., Pentzien, S., Höhm, S., Rosenfeld, A., Krüger, J., 2014, Femtosecond laser-induced periodic surface structures on steel and titanium alloy for tribological applications, Appl. Phys. A 117, p.103-110

Debord, B., Alharbi, M., Vincetti, L., Husakou, A., Fourcade-Dutin, C., Hoenninger, C., Mottay, E., Gérôme, F., Benabid, F., 2014, Multi-meter fiber-delivery and pulse selfcompression of milli-Joule femtosecond laser and fiber-aided laser-micromachining, Opt. Exp. Vol. 22, p. 10735

Eilzer, S., Funck, M. C., Wedel, B., 2016, Industrial fiber beam delivery system for ultrafast lasers: applications and recent advances, Proc. of SPIE, Vol. 9741

Eilzer, S., Funck, M. C., Wedel, B., 2017, Analysis of ultrafast material processing using flexible beam delivery, Proc. of SPIE, Vol. 10094

Funck, M. C., Eilzer, S., Wedel, B., 2017, Ultrafast fiber beam delivery – system technology and industrial application, Proc. of SPIE, Vol 10097

Gérôme, F., Cook, K., George, A.K., Wadsworth, W.J., Knight, J.C., 2007, Delivery of sub-100fs pulses through 8m of hollow-core fiber using soliton compression, Opt. Exp., Vol. 15, p. 7126

Jaeggi, B., Neuenschwander, B., Hunziker, U., Zuercher, J., Meier, T., Zimmermann, M., Selbmann, H., Hennig, G., 2012, Ultra-high-precision surface structuring by synchronizing a galvo scanner with an ultra-short-pulsed laser system in MOPA arrangement, Proc. of SPIE, Vol 8243

Neuenschwander, B., Bucher, G. F., Hennig, G., Nussbaum, C., Joss, B., Muralt, M., Zehnder, S., Hunziker, U., Schuetz, P., 2010, Processing of Dielectric Materials and Metals with ps Laserpulses, ICALEO, Paper M101

Pricking, S., Welp, P., Overbuschmann, J., Nutsch, S., Gebs, R., Fleischhaker, R., Kleinbauer, J., Wolf, M., Budnicki, A., Sutter, D. H., Killi, A., Mielke, M., 2016, Industrial grade fiber-coupled laser systems delivering ultrashort high-power pulses for micromachining, Proc. of SPIE, Vol. 9741

PT Photonic Tools GmbH, http://www.photonic-tools.de/files/ds_llk_ukp.pdf

Raciukaitis, G., Brikas, M., Gecys, P., Voisiat, B., Gedvilas, M., 2009, Use of High Repetition Rate and High Power Lasers in Microfabrication: How to keep Efficiency High ?, JLMN Journal of Laser Micro/Nanoengineering, Vol. 4(3), p. 186

Tauer, J., Orban, F., Kofler, H., Fedotov, A.B. Fedotov, I.V. Mitrokhin,V.P., Zheltikov, A.M., Wintner, E, 2007, High-throughput of single high-power laser pulses by hollow photonic band gap fibers, Laser Phys. Letters, pp. 444–448

Zimmermann, M., Jaeggi, B., Neuenschwander, B., 2015, Improvements in ultra-high precision surface structuring using synchronized galvo or polygon scanner with a laser in MOPA arrangement, Proc. of SPIE, Vol. 9350